Visualizing the near-field coupling and interference of bonding and anti-bonding modes in infrared dimer nanoantennas

Pablo Alonso-González[1]*, Pablo Albella[2], Federico Golmar[1,3], Libe Arzubiaga[1], Félix Casanova[1,4], Luis E. Hueso[1,4], Javier Aizpurua[2], and Rainer Hillenbrand[1,4]

[1]CIC nanoGUNE Consolider, 20018 Donostia – San Sebastian, Spain

[2]Centro de Fisica de Materiales (CSIC-UPV/EHU) and Donostia International Physics Center (DIPC), 20018 Donostia-San Sebastián, Spain

[3]I.N.T.I.–CONICET, Av. Gral. Paz 5445, Ed. 42, B1650JKA, San Martín, Bs As, Argentina

[4]IKERBASQUE, Basque Foundation for Science, 48011 Bilbao, Spain

*palonso@nanogune.eu

Abstract

In this talk we will show the direct visualization and identification of capacitive coupling of infrared dimer antennas in the near field by employing scattering-type scanning near-field optical microscopy (s-SNOM)[1]. The coupling is identified by (i) resolving the strongly enhanced nano-localized near fields in the antenna gap (Figure 1) and by (ii) tracing the red shift of the dimer resonance when compared to the resonance of the single antenna constituents (Figure 2). Furthermore, by modifying the illumination geometry we break the symmetry, providing a means to excite both the bonding and the "dark" anti-bonding modes. By spectrally matching both modes, their interference yields striking net enhancement or suppression of the near fields at specific locations, which could be useful in nanoscale coherent control applications.

References

[1] P.Alonso-González, P. Albella, F. Golmar, L. Arzubiaga, F.Casanova, L. E. Hueso, J. Aizpurua, and R. Hillenbrand. Optics Express, **21(1)** (2013) 1270.

Figures

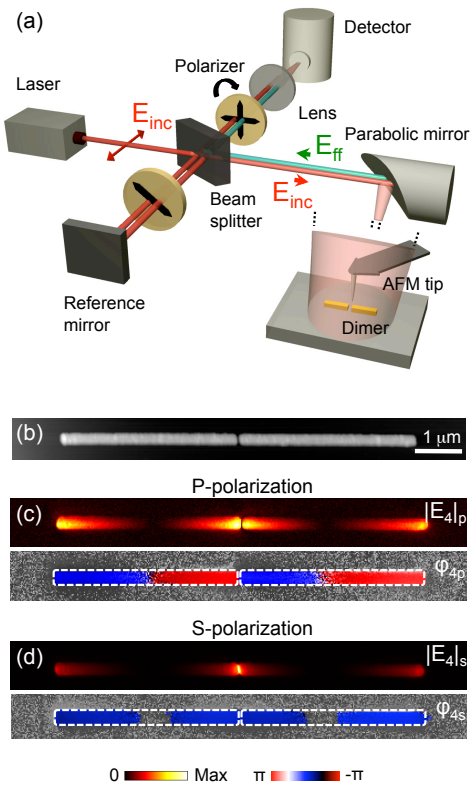

Figure 1. Experimental set-up and near-field imaging. (a) Illustration of the s-SNOM used for mapping the near-field distribution and topography of infrared dimers. The Si tip, which vibrates at the mechanical resonance frequency Ω of the AFM cantilever, is used to scatter the antenna fields. Using a parabolic mirror objective, the dimer is illuminated with the focused beam of a CO_2 laser (E_{inc}), which is polarized parallel to the long axis of the antennas (s-polarization). The same objective is used to collect the backscattered light (E_{ff}). A polarizer in front of the detector ensures the selection of either s-polarized or p-polarized backscattered fields. Signal demodulation at higher harmonics nΩ in combination with a pseudo-heterodyne interferometric detection yields background-free near-field amplitude $|E_n|$ and phase φ_n maps. (b) Topography and near-field images of a dimer antenna for (c) p-polarization ($|E_4|_p$, φ_{4p}) and (d) s-polarization ($|E_4|_s$, φ_{4s}) detection schemes. The imaging wavelength is λ_{inc} = 11.1 μm. The dashed white line in the phase images highlight the nanorods contour.

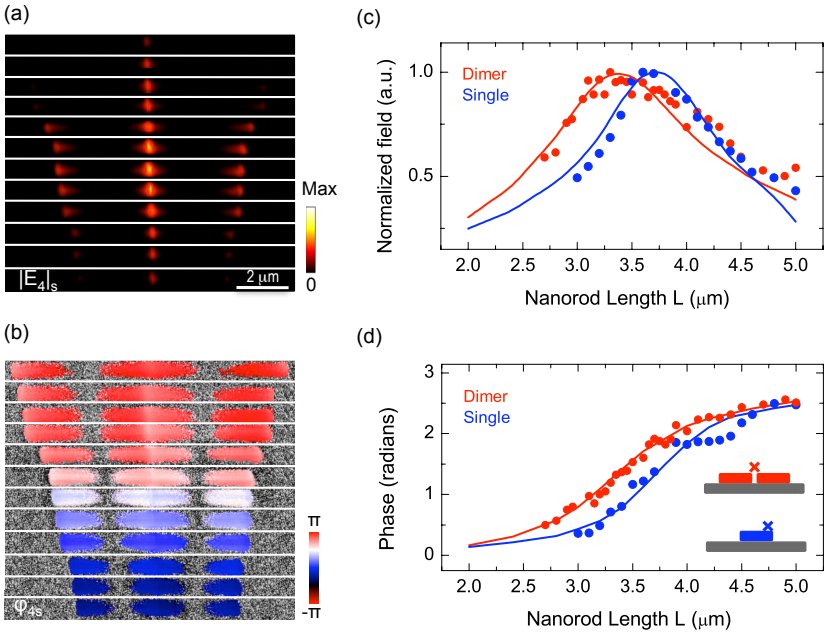

Figure 2. Verification of near-field coupling in dimer antennas. (a) Near-field amplitude $|E_4|_s$ and (b) phase φ_{4s} images of dimer antennas with a varying length L. The horizontal white lines separate the images taken individually. (c) Comparison of the normalized near-field amplitude $\sqrt{E_{4s}}$ in dimer antennas (red dots) and single nanorods (blue dots) as a function of nanorod length L. (d) Comparison of the near-field phase $\varphi_{4s}/2$ in dimer antennas (red dots) and single nanorods (blue dots) as a function of nanorod length L. The crosses in the antenna schematics show the locations were the fields were evaluated: the center of the gap for the dimers and the nanorod extremity for the single nanorods. Numerical calculations by FDTD of the in-plane component of the antennas´s near-field amplitude and phase are also shown in (c) and (d) by red (dimers) and blue (single nanorods) solid lines.